Visible and Infrared Photometry of Fourteen Kuiper Belt Objects

John K. Davies

Joint Astronomy Centre, 660 N A'ohoku Pl., Hilo, Hawaii, 96720, USA

E-mail: JKD@jach.hawaii.edu

Simon Green & Neil McBride

Unit for Space Sciences & Astrophysics, School of Physical Sciences,

University of Kent, Canterbury, CT2 7NR, UK

Erica Muzzerall *

Joint Astronomy Centre, 660 N A'ohoku Pl., Hilo, Hawaii, 96720, USA

David J. Tholen & Robert J. Whiteley

Institute for Astronomy, Woodlawn Dr, Honolulu, Hawaii, 96822 USA

Michael J. Foster & Jon K. Hillier

Unit for Space Sciences & Astrophysics, School of Physical Sciences,

University of Kent, Canterbury, CT2 7NR, UK

March 14, 2000

Number of pages (inc Figs. and Tables): 32

Tables: 5 - some more than 1 page long

Figures: 4

.

*Present address: Dept of Physics and Astronomy,University of Victoria, Box 3055, Victoria, B.C., V8W 3P6, Canada

We present V–J colors of 14 Kuiper Belt objects using new infrared (J) data combined, in most cases, with simultaneous visible (V) data. We confirm the V–J vs absolute magnitude relation reported by Jewitt & Luu (1998) for the five objects in their dataset but demonstrate that the relationship does not hold for a larger sample. Kuiper Belt objects exhibit a wide range of V–J colors but there is no correlation with heliocentric distance or orbital class. The bi-modality seen in BVR colors by Tegler & Romanishin (1998) is not present in optical-infrared colors.

Keywords. Kuiper Belt Objects, Photometry, Infrared, Visible, Centaurs.

1 INTRODUCTION

The Kuiper belt [1] comprises three dynamical classes of planetesimals close to or beyond the orbit of Neptune. Objects in the 3:2 mean motion resonance with Neptune have been described as "Pluto Type" (Marsden 1996) or more commonly "Plutinos" (Jewitt & Luu 1996), those beyond about 41 AU as "Cubewanos" (Marsden 1997) or "Classical Kuiper Belt Objects", and those with a much larger semi-major axis and higher eccentricity than the Plutinos and Classical Kuiper Belt Objects are known as Scattered Disk Objects (Luu *et al.* 1997). There are to date only a few members known of this latter class (of which 1996 TL_{66} is the brightest) although they are probably the harbingers of a much larger and more significant population.

The Kuiper belt is believed to be the source region for the outer planet crossing objects known as Centaurs and for the population of short period comets. Photometric (*e.g.* Lebofsky *et al.* 1984; Hartmann *et al.* 1988; Luu & Jewitt, 1990; Mueller *et al.* 1992; Luu & Jewitt 1996a; Davies *et al.* 1996; Romanishin *et al.* 1997, Davies *et al.* (1998a)) and spectroscopic (*e.g.* Fink *et al* 1992; Davies *et al.* 1993; Luu *et al.* 1994) observations have shown that there is considerable diversity amongst the Centaurs ranging from 2060 Chiron, which is active and has neutral colors, to 5145 Pholus which is extremely red and has unique spectral features. Luu & Jewitt (1996a) showed that the range of BVRI colors amongst the Centaurs is similar to that amongst the Kuiper Belt Objects (henceforth KBOs). Jewitt & Luu (1998) extended this work by presenting VRIJHK data for 5 KBOs which showed a wide range of visual-infrared colors similar to the visual-infrared

[1] Note that Edgeworth-Kuiper Belt may be more appropriate since Edgeworth (1943) suggested the existence of "a very large number of comparatively small bodies beyond the orbits of the planets"

colors of the Centaurs. They also found what appeared to be a linear relationship between the V−J color and absolute red magnitude, M_R, of the five KBOs in their sample. Although such a relationship could be explained in terms of larger objects preferentially retaining ices, we set out to extend the sample to test if this result was either a fluke or some form of observational artifact. Since both Jewitt & Luu (1998) and Davies *et al.* (1998a) have shown that the JHK colors of both KBOs and Centaurs are fairly neutral and that most of the color diversity is apparent between V and J, we restricted ourselves to V−J colors.

It has been shown that at least some KBOs have what appear to be rotational lightcurves (Romanishin & Tegler 1999) and this complicates the derivation of optical-IR colors unless the data are obtained simultaneously. Where possible we have arranged truly simultaneous optical and IR observations and when this has not been possible we have made repeated infrared observations over periods of days or months. The purpose of these repeated observations is to minimise the effects of any rotational lightcurves on the uncertainty in the V−J colors which we derive. In this paper we present the results of this program as applied to 14 KBOs and offer our conclusions on the issue of the spectral diversity of this population and the proposed V−J vs M_R relationship.

2 OBSERVATIONS AND DATA REDUCTION

2.1 Visible Observations

The visible data presented here were all acquired with the University of Hawaii 2.24-m telescope on 1998 Sep. 23-25 and 1999 Jan. 17-18, UT. The instrument used was the Tektronix 2048x2048 CCD camera mounted at the telescope's f/10 focus with a pixel scale of 0.219 arcsec/pixel. The observations were carried out in 2x2 binning mode. The nights were all photometric at the 1-2% accuracy level, with seeing in the 0.9" to 1.3" range. The integrations were typically 450 sec. through a standard V-filter, although exposures for some of the brighter objects were 300 sec. Standard bias removal and flat fielding techniques were employed. Repeated observations were made on each object, and each image was examined in detail to check for low surface brightness background sources and cosmic ray contamination. The amount of time spent observing a target was timed to coincide as closely as possible with the infrared observations being done at UKIRT. Normally, each block of observations spanned approximately 30 minutes. Standard aperture photometry was performed on the KBOs using the DAOPHOT package in IRAF. The aperture size for our object measurements was 12 pixels in diameter, which in 2x2 binning mode is 5.2 " on the sky. We employed standard star measurements on multiple fields taken from Landolt (1992). From these we performed full solutions for extinction coefficient, color term and magnitude zero point, all of which proved to be close to the previously measured values. The total calibration error for any given observation is mostly contained in the error on the magnitude zero point, which for the September 23-25 data is ± 0.005 magnitudes. The dominant source of error in these data is photon noise in the object measurements themselves.

Since our photometric coefficients were defined for stellar measurements made with 20 pixel apertures (8.8 "), aperture corrections were necessary. The aperture correction between the 20 pixel and 12 pixel aperture was usually between 0.04 and 0.05 magnitudes, and typically resulted in about a factor of 2 decrease in the photometric error on the object measurement. It would have been possible to use smaller apertures for these measurements however the size of the object apertures were not reduced further since the KBOs were moving during the exposures and so their PSFs were not strictly identical to those of the bright background stars and the visible wavelength measurements presented here already have error bars comparable to or smaller than their infrared counterparts. Even significant reductions in the size of the visible wavelength uncertainties would therefore not appreciably change the errors on the final (V$-$J) colors.

2.2 Infrared photometry

All the infrared photometry presented here was obtained between 1996 and early 1999 with the infrared camera IRCAM on the 3.8m UK Infrared Telescope, UKIRT. IRCAM is fitted with a 256$\times$256 InSb array (0.286 arcsec pixels, field of view of 73.2 arcsec) and an image for a given filter comprised a mosaic of several separate frames each with exposure times set to be background limited. The mosaics comprised 9 or 13 frames totalling 60s of exposure per frame and each frame was offset from the others (by between 4 and 15 arc seconds) to minimize the effect of bad pixels and to allow the production of a flat field by median filtering. All the observations were made guiding at the sidereal rate to take advantage of the improved image quality when using UKIRT's tip-tilt guider.

After subtracting an appropriate dark, frames in each filter were median filtered to produce a flat field, divided by this flat field and then mosaiced together using the STARLINK package CCDPACK. This package offers improvements over the IRCAM data reduction package used in our earlier work since during the mosaicking process CCDPACK centroids on objects within each frame to ensure maximum fidelity in the subsequent image registration.

Including overheads for slewing the telescope and reading out the array, a typical 9 position mosaic took approximately 10 minutes to complete. During this period a KBO observed at opposition moves approximately 0.4 arcsec on the sky. Since this is comparable with the pixel size, no further correction for the KBO motion was made at this stage. Between 2 and 4, normally 3, consecutive 10 minute mosaics were made on a single target before moving the telescope to observe either a standard star or another KBO. The KBO field was usually re-imaged with a further set of mosaics 2-3 hours later. These repeated observations, having total integration times of 18-36 min, served a number of purposes including allowing confirmation of the identification of the KBO by its motion and allowing the object to move to a different region of both the detector and sky to minimise any systematic errors due to bad pixels or unresolved background objects. In the case of the fainter objects, which were not reliably detected in 36 min, additional mosaics were done before moving to another source. Note that on 1997 November 22 this strategy was not followed. On this date only, single 9 position mosaics were taken at approximately 2hr intervals throughout the night. For this date the precision of the date given in table II is reduced accordingly since it does not correspond the mid-time of a specific observation, but of the period during which several mosaics were made.

If the KBO was visible in the individual 9 (or 13) position mosaics then aperture photometry was performed directly on each mosaic. In the case of the fainter objects, a number of mosaics were co-added in the asteroid's reference frame to improve the signal to noise ratio in the final image before the aperture photometry was performed.

To reduce the sky noise when performing aperture photometry on the KBO we experimented with smaller software apertures than we have used when observing brighter moving objects. We used both 2 and 3 arcsec diameter software apertures using the *STARLINK* data reduction package GAIA, which centroids on each object before calculating the counts in the selected aperture. The sky background is determined using a clipped mean (ie determining the mean and standard deviation, removing values more than $\pm$ 2 σ from that mean then re-computing the mean) of the value in an annulus extending from 7 to 15 arcsec around the target.

To deduce the appropriate aperture corrections required to calibrate the KBO photometry with images of UKIRT standard stars measured in a 5 arcsec aperture, photometry was performed on relatively bright point-like reference objects in each KBO mosaic using a range of apertures from 2 to 7 arcsec. Examination of many mosaics showed that once the aperture size had reached the 5 arcsec (17 pixels) diameter chosen for the standards then the measured magnitude was well defined and increasing the aperture still further did not change the resulting value within the increased scatter of the data. For KBO mosaics containing 2 or more reference stars, the aperture corrections from large to small apertures were the same for each star, confirming that image quality was constant across the entire IRCAM field of view.

Since the KBO was moving, and so had a slightly different point spread function from the stellar images the larger (3 arcsec) aperture was used for the asteroid photometry as in this case the aperture correction was significantly smaller than for the 2 arcsec case. Even though this choice introduces additional random noise into the photometry, the result is less subject to systematic errors due to mismatches between the stellar and KBO point spread functions. The aperture corrections from 3 to 5 arcsec ranged from -0.05 to -0.3 mag, but were not always consistent even for observations of the same field taken at different times of the night. We attribute this to changes in the intrinsic image quality (seeing) and small differences in the mosaicing process. Note that occasionally no suitable star was available since the IRCAM field of view is relatively small (approximately 73 arcseconds square) and in these cases we used the aperture corrections obtained from a 9-frame mosaic of a separate KBO taken on the same night. On the nights when this procedure was necessary, the aperture corrections from several mosiacs were examined to check that the corrections were reasonably similar from one mosaic to the next. However, in the case that there were no other 9-frame mosaics available to provide suitable aperture corrections, or there was evidence that the image quality varied considerably with time, we used a 5 arcsec aperture only, did not perform an aperture correction, and accepted the higher random error.

Photometric calibration was performed via observations of UKIRT faint standard stars listed at http://www.jach.hawaii.edu/JACpublic/UKIRT/astronomy/calib/faint_stds.html. Note that some of these values will shortly be revised at the few hundreths of a magnitude level but that the updated values, provided to us by T.G.Hawarden (Private Communication) were used here. The quoted errors are dominated by statistical uncertainties in the images rather than uncertainties in the photometric calibration. Observational details and individual J magnitudes are given in Table II. The times are for the mid point of the total observation (ie the set of several consecutive mosaics) and are not corrected for light travel time. Some images were taken on nights when the presence of cirrus clouds made conditions unsuitable for photometry. In such circumstances the fields were re-observed on other, photometric, nights to allow photometric calibration via stars in the images.

3 RESULTS

3.1 Optical Photometry

The optical photometry from the University of Hawaii 2.24m telescope is presented in Table I. Since these values may be of interest for other purposes, and provide an idea of the internal consistency of the data, we provide the entire set of values without averaging. The times are mid-exposure with no light travel time correction. For each repeated group of observations of a single object we also present the observing geometry.

3.2 Infrared Photometry

The infrared photometry is provided in Table II. In this case we have treated each observation of a single object as a single data point, irrespective of whether the object was bright enough to extract photometry from individual mosaics of the final dataset. They are thus all, in effect, values from long integrations with effective exposure times of between 18 and 108 min. When we obtained multiple values from consecutive mosaics these have been averaged using a weighted mean value and the quoted error includes the internal scatter of the values put into the mean. The quoted time marks the approximate time of the middle of the exposure, with no light travel time correction

3.3 Derivation of Visible-Infrared Colors

Since we have noted that at least some KBOs have what appear to be rotational lightcurves, to derive V$-$J colors data over the whole wavelength range should be obtained simultaneously, or at least within a period of a few minutes. Whenever possible this was done by co-ordinating observations from the UKIRT and University of Hawaii 2.24m telescope on Mauna Kea. When no simultaneous observations were available, we deduced the V magnitude at the time of the infrared observation using an assumed value of 0.15 for the phase curve slope parameter G. The values of H_V for the one object not observed by us in V was provided by the Minor Planet Center through the MPECs. The likely error introduced when correcting between phase angles typical of the observations reported here is $\pm$ 0.02 mag with the worst case $\pm$0.05 mag (assuming G in the range 0.05–0.25) and this is small compared with the other uncertainties. The values of H_V which we derive are generally similar to that of other workers (see Table III). Note that we used the optical data presented by Jewitt and Luu (1998) to compute a value of H_V for Table III but did not use this in any of our V magnitude estimates in order to make our result completely independent of their dataset. The value of V used for calculation of the V−J color is given in Table IV.

4 DISCUSSION

We present our deduced values of V−J for each observation in Table IV which indicates both the number of data points per object and gives an idea of the internal consistency of our results. For ease of further discussion we then combine these via a weighted mean into a single value for the V−J of each object in Table V. This table also shows some orbital information and the V−J values of Jewitt & Luu (1998) for comparison with our data.

We find that the V−J colors for three out of five objects common to this work and Jewitt & Luu (1998) agree within the formal errors and in the case of 1996 TO_{66} the values differ by 0.28mag, or about 3 standard deviations. The major disagreement is in the case of 1993 SC, where the difference is of order 0.6mag, or 7.5 standard deviations. Davies *et al.* (1997) presented a value of V−J for 1993SC of 2.08 $\pm$0.17 which is consistent with the value of 1.97 $\pm$0.08 advanced by Jewitt & Luu (1998). However the V−J color presented by Davies *et al.* (1997) is based on non-simultaneous data and relies on a V magnitude extracted from a single observation and combined with three values of J from different nights. We find that the J values of Davies *et al.* (1997) are quite consistent with the J data presented here, for example the average J value from September 1998 is 0.03 magnitudes fainter than that from September 1995, when the the effects of changing Sun-KBO-Earth distance would predict a fading by 0.06 magnitudes. However, the single V value from 1995 is some 0.3 magnitudes brighter than would be expected based on the H_V presented here. Tegler & Romanishin (1997) and Davies *et al.* (1997) have shown that 1993SC does not have a lightcurve amplitude large enough to explain a change of 0.3 mag and, while the sense of the error is such that an outburst of some kind could be invoked to explain the 1995 V data, we note that Davies *et al.* (1997) stated that the magnitudes which they obtained were different depending on whether they used aperture photometry or profile fitting techniques. Furthermore these differences were most extreme in the case of the V frame where the V profile “showed a very poor fit to the PSF derived from field stars”. Thus we suggest that the V value derived from this 1995 image may be in error, perhaps due to contamination by a faint background object. Using the value of H_V presented in this paper to deduce the V in September 1995 would give a V magnitude of 22.65. This revision in the V magnitude would give V−R and V−I values for 1993 SC in closer agreement with those of Luu & Jewitt (1996b), Jewitt & Luu (1998) and Tegler *et al.* (1997) and a revised value of V−J of 2.38± 0.17 in 1995. This value would be in agreement with the V−J deduced by us using our 1998 data, although it would weaken the agreement between the 1995 V−J color data and the 1997 data of Jewitt & Luu (1998).

Note also that while the average V−J color of 1996 TL_{66} quoted in Table V is in formal agreement with data of Jewitt & Luu (1998) the internal scatter in the data presented here is larger than the formal errors would suggest. The value of H_V which we derive is quite consistent between our data and Jewitt & Luu (1998), the differences stem from the scatter in our J data for which we have no explanation. There have been two reports which suggest cometary activity in KBOs, Fletcher *et al.* (1998) reported a cometary coma around 1994 TB and Hainaut *et al.* (1999) report changes in the details of the rotational lightcurve of 1999 TO_{66} which they attribute to an outburst. While we cannot rule out activity as an explanation of the scatter in our V−J color (since we only have simultaneous V data for a single date) the sense of the changes do not seem consistent with an outburst affecting our J data. If the UKIRT data were taken when the object had a coma this would make the J magnitude numerically smaller and so increase the value of V−J, but the opposite effect is observed. Brown *et al.* (1999) have shown that 1996 TO_{66} has water ice absorption features which may vary from night to night suggesting a patchy surface, but to explain the 1996 TL_{66} data presented here would require surface materials having identical reflectivity in V but quite different reflectivity at J. We are reluctant to advance this as an explanation since the optical-infrared spectrum of 1996 TL_{66} presented by Luu & Jewitt (1998) is featureless across the J band.

The BVRI and visible–IR colors, and the possible relationships between them, of various outer solar system objects have been discussed extensively in several recent papers (*e.g.* Luu & Jewitt 1996a; Weintraub *et al.* 1997; Davies *et al.* 1998b) and for conciseness this discussion will not be repeated here. Issues which can be addressed with the dataset presented here include;

i) are the visible–infrared colors of the KBOs similar to those of the Centaurs?

ii) is there a linear relationship between V−J and absolute magnitude?

iii) are there any trends in surface composition, as deduced from visible–IR colors, with heliocentric distance?

iv) is the bimodal distribution of colors seen in the BVR plane by Tegler & Romanishin (1998) evident in V−J?

Luu & Jewitt (1996a) argued on the basis of visible colors alone that the Kuiper Belt comprises objects with a range of surface properties and similar conclusions were presented by Green *et al.* (1997). However, Tegler & Romanishin (1998) showed on the basis of BVR colors that these distant objects form a bi-modal population with one group of objects being only slightly redder than the Sun while the others are very red indeed and that the two groups are well separated in the BVR plane.

Few visible–IR colors have been presented for KBOs other than those of 1993 SC (Davies *et al.* 1997) and the five objects in Jewitt & Luu (1998). Jewitt & Luu (1998) find "extreme differences, especially in the measured V−J color indices, that indicate a wide range of surface compositions in the Kuiper Belt" but, while referring to some objects as spectral analogues of 2060 Chiron and others as more closely resembling 5145 Pholus, they do not argue specifically for a bimodal distribution. The new V−J colors of KBOs presented here do not represent a bimodal distribution but show a wide range of colors supporting the view of Luu & Jewitt that they are indistinguishable on this basis from Centaurs.

Our recent V−J colors of 2.57 for 1993 SC and 2.54 for 1994 TB make these objects as red as the Centaur 5145 Pholus, which has a V−J of 2.58. This conclusion of the extreme redness of these two Kuiper Belt Objects was also reached by Tegler & Romanishin (1997) based on BVR data. Pholus has a number of spectral features in the near IR (Davies *et al.* 1993, Luu, Jewitt and Cloutis 1994) which Cruikshank *et al.* (1998) attribute to "small hydrocarbons" akin to methanol and its photochemical products. While the spectum of Pholus is not identical to that of 1993 SC, Brown *et al.* (1997) have suggested that this object too has simple hydrocarbons on its surface.

Jewitt & Luu (1998) present a linear relationship between V−J and absolute red magnitude M_R for five Kuiper belt objects which has a linear correlation coefficient of 0.981. If M_R is related directly to size, this implies that the smaller objects are systematically redder. We have tested this relationship with our new data by plotting V−J vs H_V (which should be directly related to size assuming constant albedo) and find that while our dataset is completely independent of theirs for the 5 objects in their dataset (except in so far as the optical data is taken from the same telescope) we obtain exactly the same result (Fig 1) i.e. that the 5 KBO's fall on a line with a high linear correlation co-efficent (0.958 in our case) between V$-$J and absolute magnitude. This effectively removes any possiblity that the relationship reported by Jewitt & Luu (1998) is caused by any systematic effect in the data reduction methodology.

However when our complete dataset is considered the picture is not as clear. If we pick the other 6 objects for which we have good detections it is possible to fit a straight line but this has significantly poorer correlation coefficent (0.538) and different values of both slope and intercept from the line plotted in Fig 1. The entire dataset, including 2 upper limits and one object for which we obtained a low signal-to-noise detection on one night and upper limits on another is shown in Fig 2. For the 11 objects for which we have reliable detections there does appear to be a general trend of increasing redness with reducing size (assuming near constant albedos) but the correlation is not as tight as before. Perhaps more significantly the three objects for which we have only weak detections or upper limits fall below the general trend, suggesting that they are small, blue objects with colors more akin to 2060 Chiron.

We now consider this result in terms of detection efficiency. Large objects, ie those with small values of H_V, will be detectable over a wide range of distances irrespective of their V$-$J color. However, as the H_V increases and the V magnitude increases (ie the object becomes fainter) for a given observing condition, those objects with large V$-$J's will be more detectable in the infrared. We have attempted to show this effect in Fig 3 in which we plot diagonal lines of constant detectability against distance and H_V. This shows that large objects can be detected at UKIRT in approximately 20min of integration whatever their color, but that small objects, even if relatively close to the Sun, are only detectable if they have red V$-$J colors. Thus we would not expect to detect even nearby objects having H_V greater than 8 unless their V$-$J color was greater than about 2. Accordingly populating the lower right hand corner of Fig 2 with detections from UKIRT is difficult and indeed this region of the diagram contains only low s/n detections and upper limits. The lack of a detection of an object in the upper left of Fig 2 may be interpreted in one of two ways. It may be an artifact of the small sample size (large objects are rare and a large red object may not yet have been found) or perhaps larger objects at least are preferentially blue.

Eckholm *et al.* (1999) reported that they could find no trend of V$-$I color with M_R (indeed they reported that 6 of 7 objects in their sample suggested quite the opposite trend but since

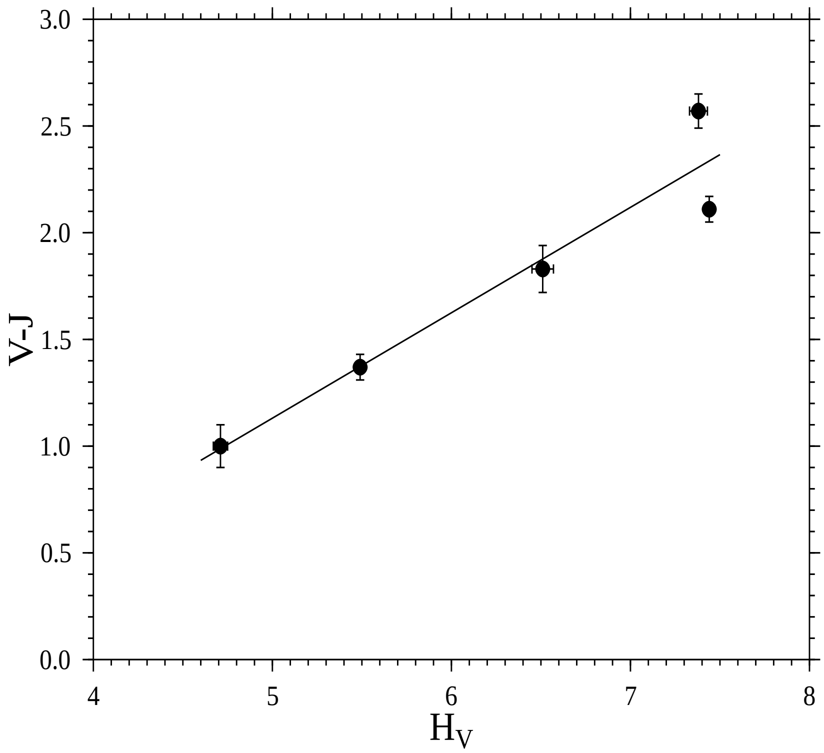

Figure 1: Our values of V−J color vs absolute visual magnitude (H_V) for the five KBOs observed by Jewitt & Luu (1998). These exhibit the same color-magnitude relationship which they reported.

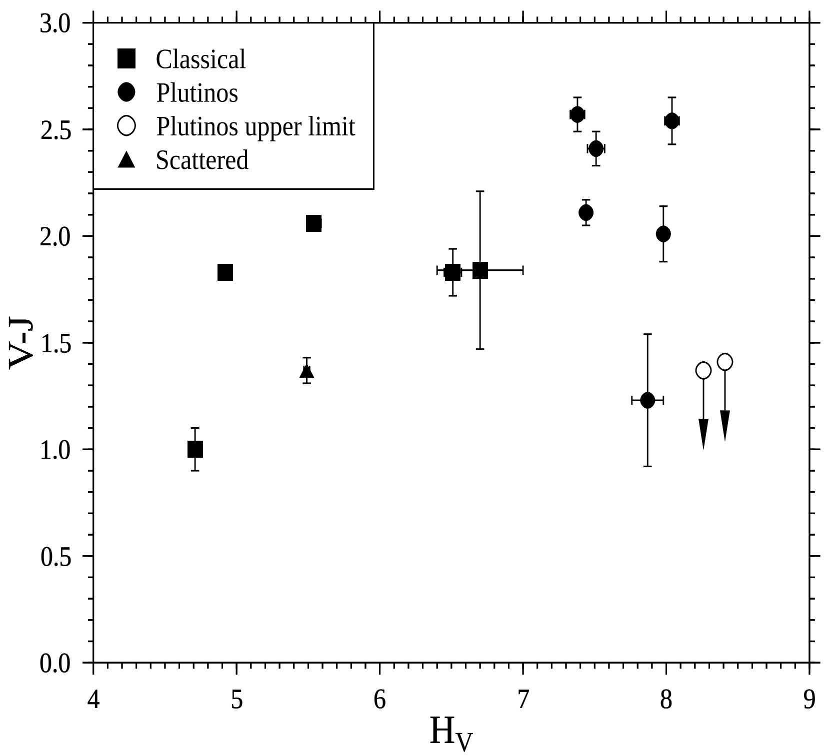

Figure 2: V−J color vs absolute visual magnitude (H_V) for 14 KBOs. No strong correlation is apparent.

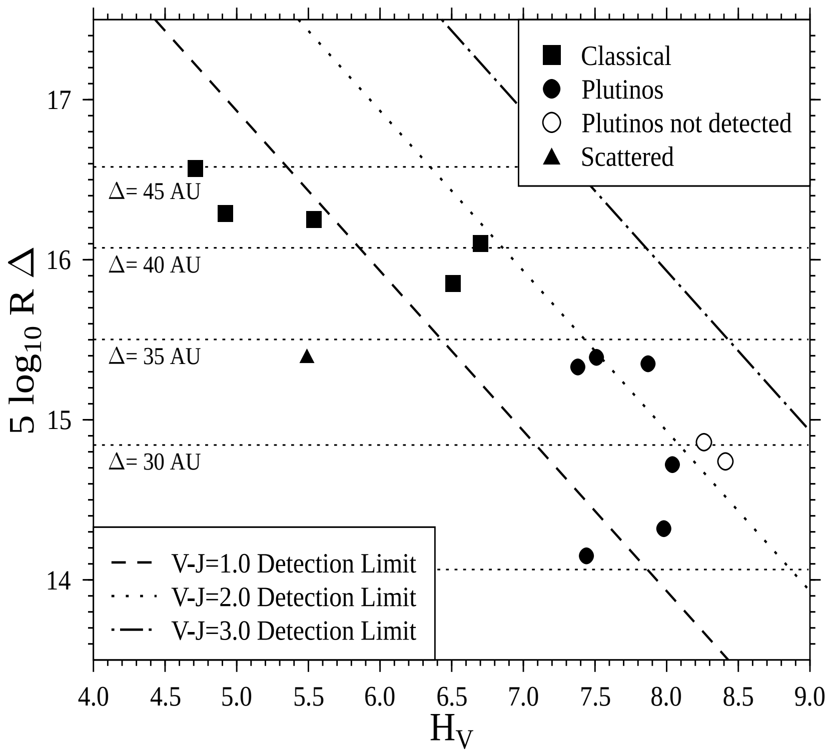

Figure 3: Figure 3. This figure gives an indication as to whether we would expect to detect any particular Kuiper Belt Object with a given absolute visual magnitude, heliocentric and geocentric distance. The diagonal lines represent UKIRT detection thresholds, based on a 3 sigma detection after an exposure of 18 minutes (about twice our typical mosaicked frame) as quoted in the IRCAM sensitivity tables. For example, an object with V−J=2.0 can only be detected if it lies to the lower left of the V−J=2.0 diagonal line. Also shown are horizontal dotted lines indicating lines of equal geocentric distance (assuming observation at opposition).

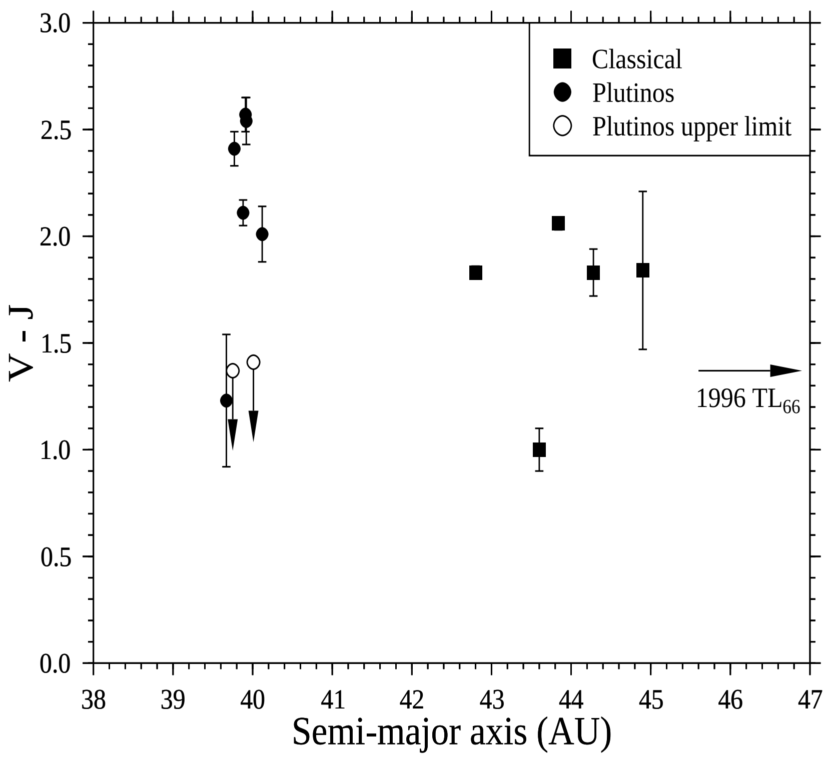

Figure 4: Figure 4. V−J color vs semi-major axis for 14 KBOs. No correlation is apparent.

the 7th was not consistent with this slope they rejected this apparent relationship as a fluke). However they did comment that the V−I color of the 7 KBOs in their sample showed a strong likelihood of correlating with semi-major axis (the significance of this correlation was quoted as 99%). That this relationship is not generally true can be seen by considering either the colors of 1996 TL_{66} which has intermediate V−I (eg Jewitt and Luu 1998) but a semi-major axis of 85AU, or the V−J colors presented here which show no such relationship (Fig 4).

5 CONCLUSIONS

The KBO's have a wide range of V−J colors and these are not correlated with orbital class.

The apparent trend of increasing V−J with H_V appears to be a result of selection effects due to difficulty of detecting small, blue objects and the small number of large objects so far discovered.

There is no convincing trend of increasing redness with semi-major axis amongst the KBOs studied so far.

There is no bi-modality of V−J colors which seem to range smoothly from approximately 1 to 2.6.

ACKNOWLEDGEMENTS

UKIRT is operated by the Joint Astronomy Centre, on behalf of the UK Particle Physics and Astronomy Research Council (PPARC). Image processing and data reduction were performed using the STARLINK network and software. STARLINK is funded by PPARC. N. McBride, M. Foster and J. Hillier acknowledge the financial support of PPARC. D. Tholen and R. Whiteley acknowledge support from NASA Grant NAG 5-4524

REFERENCES

Brown, R.H, Cruikshank, D.P., Pendleton, Y., Veeder, G.J. (1997): Surface composition of Kuiper Belt object 1993 SC. *Science* **276** 937-939

Brown, R.H., Cruikshank, D.P. and Pendleton, Y. 1999. Water ice on Kuiper Belt Object 1996 TO_{66} *Ap. J.* 519 L101-104.

Cruikshank, D.P. and 15 colleagues. (1998) The composition of Centaur Pholus. *Icarus* **135**, 389-407

Davies, J.K., M.V. Sykes and D.P. Cruikshank 1993. Near infrared photometry and spectroscopy of the unusual minor planet 5145 Pholus (1992AD). *Icarus* **102**, 166–169.

Davies, J.K., D.J. Tholen and D.R. Ballantyne 1996. Infrared observations of distant asteroids. In *Completing the Inventory of the Solar System*, ASP Conference Proceedings (T.W. Rettig and J.M. Hahn, Eds.), **107**, pp. 97–105, ASP, San Francisco.

Davies, J.K., N. McBride and S.F. Green 1997. Optical and infrared photometry of Kuiper Belt object 1993 SC. *Icarus* **125**, 61-66.

Davies, J.K. McBride, N, Ellison, S.E. Green, S.F. and Ballantyne D. 1998a Visible and infrared observations of six centaurs. *Icarus* **134** 213-227

Davies, J. K., N. McBride, S.F. Green, S. Mottola, U. Carsenty, D. Basran, K.A. Hudson, and M.J. Foster 1998b. The lightcurve and colors of unusual minor planet 1996 PW. *Icarus.* **132** 418-430

Eckholm, A.G., M. Dahlgren, C-I. Lagerkvist, M. Lundström, P.Magnusson and J. Warell. 1999. VRI Photometry of Kuiper Belt objects and Centaurs. Paper presented at Lunar and Planetary Science Conference, March 15-19, Houston, Texas and available via http://cass.jsc.nasa.gov/meetings/LPSC99/pdf/1714.pdf

Edgeworth, K.E. 1943. The evolution of our planetary system. *J. Brit. Astron. Assoc.* **53**, 181-188.

Fletcher, E.A., A. Fitzsimmons., I.P. Williams., N Thomas, and W-H.Ip (1999). HST observations of the Kuiper Belt. in Minor Bodies of the Outer Solar System, proceedings of the MBOSS-98 meeting held at ESO garching November 1998. Eds Fitzsimmons A., West R.

Fink, U., M. Hoffmann, W. Grundy, M. Hicks and W. Sears 1992. The steep red spectrum of 1992AD: an asteroid covered with organic material? *Icarus* **97**, 145–149.

Green, S.F., N. McBride, D. O'Cealleagh, A. Fitzsimmons, M.J. Irwin and I.P. Williams 1997. Surface reflectance properties of distant solar system bodies. *Mon. Not. R. Astr. Soc.* **290**, 186–192.

Hainaut, O.R., C.E.Delahodde, H. Boehnhardt, E. Dotto, M.A. Barruchi, K.J.Meech J.M. Bauer and A Doressoundiram (1999) Physical properties of TNO 1999 TO_{66}. Submitted to A & A.

Hartmann, W.K., D.J. Tholen, K.J. Meech and D.P. Cruikshank 1990. 2060 Chiron: colorimetry and cometary behavior. *Icarus* **83**, 1–15.

Jewitt, D. and Luu, J.X. 1996. The Plutinos. In *Completing the Inventory of the Solar System*, ASP Conference Proceedings (T.W. Rettig and J.M. Hahn, Eds.), **107**, pp. 255–258, ASP, San Francisco

Jewitt, D. and J. Luu 1998. Optical–Infrared spectral diversity in the Kuiper Belt. *Astron. J.* **115** 1667-1670

Landolt, A.U., 1992, UBVRI standard stars in the magnitude range 11.5<V<16.0 around the celestial equator, *AJ* **104**, 340-376

Lebofsky, L.A., D.J. Tholen, G.H. Rieke and M.J. Lebofsky 1984. 2060 Chiron: Visual and thermal infrared observations. *Icarus* **60**, 532–537.

Luu, J. and D. Jewitt 1990. Cometary activity in 2060 Chiron. *Astron. J.* **100** 913–932.

Luu, J.X. and Jewitt, D. (1996a): Color diversity among the Centaurs and Kuiper Belt objects. *Astron. J.* **112** (5), 2310–2318

Luu, J.X. and Jewitt, D. (1996b): Reflectance Spectrum of the Kuiper belt Object 1993 SC. *Astron. J.* **111** (1), 449-503

Luu, J.X. and Jewitt, D. (1998): Optical and infrared reflectance spectrum of Kuiper Belt Object 1996 TL_{66}. *ApJ* **494** L117-121

Luu, J., D. Jewitt and E. Cloutis 1994. Near infrared spectroscopy of primitive solar system objects. *Icarus* **109**, 133–144.

Luu J.X., Marsden, B., Jewitt, D.,Trujillo, C., Hergenrother, C., Chen, J. and Offutt, W. 1997. A new dynamical class of objects in the outer Solar System. *Nature* **387**, 573

Marsden B. (1996): Searches for Planets and Comets. In *Completing the Inventory of the Solar System*, ASP Conference Proceedings (Eds. T.W. Rettig and J.M. Hahn.), **107**, pp. 193–207, ASP, San Francisco

Marsden B. (1997): M.P.E.C. 1997-P12

Mueller, B.E.A., D.J. Tholen, W.K. Hartmann and D. Cruikshank 1992. Extraordinary colors of asteroidal object (5145 Pholus) 1992AD. *Icarus* **97**, 150–154.

Romanishin, W., S.C. Tegler, J. Levine and N. Butler 1997. BVR photometry of centaur objects 1995 GO, 1993 HA_2 and 5145 Pholus. *A. J.* **113**, 1893–1898.

Romanishin, W. and Tegler, S.C. (1999). Rotation rates of Kuiper Belt objects from their lightcurves. *Nature* **398** 129-132

Tegler, S.C. and W. Romanishin 1997. The extraordinary colors of trans-Neptunian objects 1994 TB and 1993 SC. *Icarus* **126**, 212–217.

Tegler, S.C., Romanishin, W., Stone, A., Tryka, K., Fink, U. and Fevig, R. (1997): Photometry of the Trans Neptunian Object 1993 SC. *Astron. J* **114** 1230-1233

Tegler, S.C. and W. Romanishin 1998. Two distinct populations of Kuiper Belt Objects. *Nature* **392** 49-50

Weintraub, D.A., S.C. Tegler & W. Romanishin 1997. Visible and near infrared photometry of the Centaur objects 1995 GO and 5145 Pholus. *Icarus.* **128** 456-463

TABLE I

Optical Photometry from the UH 2.24m.

Object	UT	R (AU)	Δ (AU)	$\alpha°$	V Mag
1996 TQ_{66}	1998 Sep 23.39632	34.613	33.743	0.836	22.885$\pm$ 0.112
1996 TQ_{66}	1998 Sep 23.40193				22.953$\pm$ 0.114
1996 TQ_{66}	1998 Sep 23.40754				23.007$\pm$ 0.119
1996 TQ_{66}	1998 Sep 23.41315				22.882$\pm$ 0.108
1996 TQ_{66}	1998 Sep 23.41876				22.839$\pm$ 0.292
1996 TQ_{66}	1998 Sep 23.51849	34.613	33.743	0.833	23.143 $\pm$ 0.140
1996 TQ_{66}	1998 Sep 23.52410				22.951 $\pm$ 0.118
1996 TQ_{66}	1998 Sep 23.52972				23.437 $\pm$ 0.172
1996 TQ_{66}	1998 Sep 23.53533				23.272 $\pm$ 0.151
1996 TO_{66}	1998 Sep 23.54678	45.856	44.853	0.061	21.277 $\pm$ 0.031
1996 TO_{66}	1998 Sep 23.55239				21.357 $\pm$ 0.033
1996 TO_{66}	1998 Sep 23.55800				21.231 $\pm$ 0.030
1996 TS_{66}	1998 Sep 23.45205	38.835	38.060	0.950	22.682 $\pm$ 0.096
1996 TS_{66}	1998 Sep 23.45765				22.631 $\pm$ 0.088
1996 TS_{66}	1998 Sep 23.46326				22.603 $\pm$ 0.086
1996 TS_{66}	1998 Sep 23.47489				22.490 $\pm$ 0.077
1996 TS_{66}	1998 Sep 23.57205	38.835	38.060	0.95	22.512 $\pm$ 0.074
1996 TS_{66}	1998 Sep 23.57766				22.404 $\pm$ 0.122
1996 TS_{66}	1998 Sep 23.58327				22.225 $\pm$ 0.057
1996 TS_{66}	1998 Sep 23.58888				22.572 $\pm$ 0.079
1996 TS_{66}	1998 Sep 23.59450				22.460 $\pm$ 0.201
1996 TL_{66}	1998 Sep 23.48332	35.103	34.299	0.991	20.996 $\pm$ 0.021
1996 TL_{66}	1998 Sep 23.48893				21.003 $\pm$ 0.020
1996 TL_{66}	1998 Sep 23.49455				21.007 $\pm$ 0.021
1996 TL_{66}	1998 Sep 23.50016				21.022 $\pm$ 0.021
1996 TL_{66}	1998 Sep 23.50580				21.038 $\pm$ 0.021
1996 TL_{66}	1998 Sep 23.51141				21.038 $\pm$ 0.044

TABLE I Continued

Optical Photometry from the UH 2.24m.

Object	UT	R (AU)	Δ (AU)	$\alpha°$	V Mag
1996 TL_{66}	1998 Sep 23.60251	35.102	34.298	0.989	20.988 $\pm$ 0.057
1996 TL_{66}	1998 Sep 23.60812				21.011 $\pm$ 0.021
1996 TL_{66}	1998 Sep 23.61373				20.992 $\pm$ 0.021
1996 TL_{66}	1998 Sep 23.61935				21.025 $\pm$ 0.020
1993 SC	1998 Sep 24.46313	34.638	33.643	0.211	22.691 $\pm$ 0.083
1993 SC	1998 Sep 24.47455				22.903 $\pm$ 0.105
1993 SC	1998 Sep 24.48599				22.838 $\pm$ 0.091
1993 SC	1998 Sep 24.49754				22.792 $\pm$ 0.094
1993 SC	1998 Sep 24.58299	34.638	33.643	0.208	22.533 $\pm$ 0.088
1993 SC	1998 Sep 24.59445				22.633 $\pm$ 0.088
1993 SC	1998 Sep 24.60589				22.902 $\pm$ 0.108
1996 TP_{66}	1998 Sep 25.59928	26.394	25.490	0.960	21.692 $\pm$ 0.037
1996 TP_{66}	1998 Sep 25.61082				21.625 $\pm$ 0.105
1996 TP_{66}	1998 Sep 25.62221				21.733 $\pm$ 0.040
1996 TP_{66}	1998 Sep 25.63357				21.670 $\pm$ 0.048
1995 QY_9	1998 Sep 24.37673	25.575	28.601	0.467	22.731 $\pm$ 0.085
1995 QY_9	1998 Sep 24.38824				22.616 $\pm$ 0.084
1995 QY_9	1998 Sep 24.39970				22.688 $\pm$ 0.084
1995 QY_9	1998 Sep 24.41122				22.729 $\pm$ 0.089
1995 QY_9	1998 Sep 24.50541	25.575	28.601	0.472	22.784 $\pm$ 0.101
1995 QY_9	1998 Sep 24.51701				22.706 $\pm$ 0.089
1995 QY_9	1998 Sep 24.54023				22.574 $\pm$ 0.081
1994 TB	1998 Sep 24.55259	30.121	29.129	0.287	22.909 $\pm$ 0.110
1994 TB	1998 Sep 24.56412				22.713 $\pm$ 0.086
1994 TB	1998 Sep 25.50899	30.120	29.129	0.293	22.872 $\pm$ 0.108
1994 TB	1998 Sep 25.52037				22.748 $\pm$ 0.098
1994 TB	1998 Sep 25.53180				22.782 $\pm$ 0.101

TABLE I Continued

Optical Photometry from the UH 2.24m.

Object	UT	R (AU)	Δ (AU)	α°	V Mag
1996 SZ_4	1998 Sep 25.39132	30.260	29.284	0.443	23.396 $\pm$ 0.167
1996 SZ_4	1998 Sep 25.40273				23.166 $\pm$ 0.127
1996 SZ_4	1998 Sep 25.41655				23.425 $\pm$ 0.179
1996 SZ_4	1998 Sep 25.42815				23.042 $\pm$ 0.125
1993 SB	1998 Sep 25.43565	31.117	30.121	0.224	23.019 $\pm$ 0.112
1993 SB	1998 Sep 25.44715				23.297 $\pm$ 0.155
1993 SB	1998 Sep 25.45869				23.206 $\pm$ 0.139
1993 SB	1998 Sep 25.47084				23.254 $\pm$ 0.132
1993 SB	1998 Sep 25.55592	31.117	30.121	0.220	23.184 $\pm$ 0.145
1993 SB	1998 Sep 25.56735				23.153 $\pm$ 0.151
1993 SB	1998 Sep 25.57888				22.981 $\pm$ 0.120
1993 SB	1998 Sep 25.59058				23.282 $\pm$ 0.172
1997 QJ_4	1998 Sep 25.29674	34.752	33.754	0.163	23.164 $\pm$ 0.135
1997 QJ_4	1998 Sep 25.30837				23.365 $\pm$ 0.178
1997CS_{29}	1999 Jan 17.48097	43.616	42.633	0.11	22.021 $\pm$ 0.165
1997CS_{29}	1999 Jan 17.49160				22.021 $\pm$ 0.156
1997 CS_{29}	1999 Jan 18.45499	43.616	42.633	0.11	21.989 $\pm$ 0.154
1997 CS_{29}	1999 Jan 18.46497				21.990 $\pm$ 0.135
1997 CS_{29}	1999 Jan 18.48163				21.974 $\pm$ 0.099
1997 CS_{29}	1999 Jan 18.48977				21.870 $\pm$ 0.094
1997 CS_{29}	1999 Jan 18.58663	43.616	42.633	0.11	21.654 $\pm$ 0.108
1997 CS_{29}	1999 Jan 18.59132				21.822 $\pm$ 0.146
1997 CS_{29}	1999 Jan 18.60103				21.777 $\pm$ 0.125
1997 CS_{29}	1999 Jan 18.60570				22.183 $\pm$ 0.217
1997 CS_{29}	1999 Jan 18.61079				22.137 $\pm$ 0.201

TABLE I Continued

Optical Photometry from the UH 2.24m.

Object	UT	R (AU)	Δ (AU)	$\alpha°$	V Mag
1998 WH_{24}	1999 Jan 17.32030	42.748	42.265	1.155	21.262 ± 0.078
1998 WH_{24}	1999 Jan 17.33102				21.617 ± 0.121
1998 WH_{24}	1999 Jan 17.34076				21.462 ± 0.090
1998 WH_{24}	1999 Jan 17.35061				21.228 ± 0.086
1998 WH_{24}	1999 Jan 17.35530				21.394 ± 0.101
1998 WH_{24}	1999 Jan 18.31913	42.748	42.280	1.166	21.303 ± 0.076
1998 WH_{24}	1999 Jan 18.32878				21.295 ± 0.088
1998 WH_{24}	1999 Jan 18.33923				21.350 ± 0.092
1998 WH_{24}	1999 Jan 18.34513				21.524 ± 0.114

TABLE II Infrared (J) photometry from UKIRT.

Object	UT	R	Δ	α	J Mag	Notes
1993 SB	1998 Sept 25.4444	31.117	30.121	0.224	> 21.8	3σ upper limit in 36 min
1993 SC	1998 Sept 24.4716	34.638	33.643	0.211	20.330 ± 0.088	
1993 SC	1998 Sept 24.5976				20.286 ± 0.178	
1993 SC	1998 Sept 26.5333	34.639	33.640	0.154	20.187 ± 0.080	cirrus clouds - rel. photometry
1993 SC	1998 Sept 26.5932				19.937 ± 0.099	cirrus clouds - rel. photometry
						T_{int} 36 min
1994 TB	1998 Sept 24.4402	30.121	29.129	0.293	20.337 ± 0.077	T_{int} 36 min
1994 TB	1998 Sept 24.5573				20.393 ± 0.136	
1994 TB	1998 Sept 25.5364	30.120	29.129	0.293	20.254 ± 0.089	T_{int} 54 min
1995 QY_9	1998 Sept 24.4000	29.575	28.601	0.472	20.784 ± 0.123	T_{int} 36 min
1995 QY_9	1998 Sept 24.5009				20.491 ± 0.154	T_{int} 45 min
1996 SZ_4	1998 Sept 25.4145	30.260	29.284	0.443	> 21.8	3σ upper limit in 36 min
1996 TL_{66}	1997 Oct 13.3717	35.157	34.193	0.422	20.045 ± 0.080	cirrus clouds -rel. photometry
1996 TL_{66}	1997 Oct 13.6029				19.850 ± 0.082	cirrus clouds -rel. photometry
1996 TL_{66}	1997 Nov 22.36	35.150	34.260	0.709	19.734 ± 0.049	4 mosaics at 2hr intervals
1996 TL_{66}	1998 Sept 23.5027	35.013	34.299	0.991	19.655 ± 0.046	
1996 TL_{66}	1998 Sept 23.6084				19.649 ± 0.047	T_{int} 18 min
1996 TO_{66}	1998 Sept 23.4291	45.856	44.853	0.061	20.301 ± 0.067	
1996 TO_{66}	1998 Sept 23.5564				20.287 ± 0.094	
1996 TP_{66}	1997 Sept 01.5337	26.436	25.731	1.584	19.568 ± 0.058	
1996 TP_{66}	1997 Oct 13.4050	26.431	25.440	0.256	19.584 ± 0.113	cirrus clouds - rel. photometry
1996 TP_{66}	1997 Oct 13.5740				19.690 ± 0.092	cirrus clouds - rel. photometry
1996 TP_{66}	1997 Nov 22.35	26.426	25.634	1.300	19.614 ± 0.118	3 mosaics over 4.5 hr
1996 TP_{66}	1998 Sept 25.6164	26.394	25.490	0.960	19.388 ± 0.056	
1996 TQ_{66}	1998 Sept 23.4017	34.613	33.743	0.833	20.504 ± 0.099	T_{int} 36 min
1996 TQ_{66}	1998 Sept 23.5258				20.727 ± 0.118	
1996 TQ_{66}	1999 Jan 18.2272	34.614	34.591	1.628	20.851 ± 0.159	

TABLE II Continued

Infrared (J) photometry from UKIRT.

Object	UT	R	Δ	α	J Mag	Notes
1996 TS_{66}	1998 Sept 23.4633	38.835	38.060	0.950	20.736 ± 0.176	T_{int} 36 min
1996 TS_{66}	1998 Sept 23.5771				20.604 ± 0.140	T_{int} 18 min
1996 TS_{66}	1999 Jan 18.2821	38.835	38.062	0.954	20.618 ± 0.195	
1997 CQ_{29}	1999 Apr 11.3658	41.131	40.402	0.960	21.159 ± 0.221	T_{int} 108 min
1997 CS_{29}	1998 Feb 24.3403	43.612	42.860	0.853	19.997 ± 0.089	two 13 min integrations
1997 CS_{29}	1998 Feb 24.4233				20.001 ± 0.131	T_{int} 13 min
1997 CS_{29}	1998 Feb 24.4902				19.923 ± 0.092	two 13 min integrations
1997 CS_{29}	1998 Feb 25.3019	43.612	42.871	0.870	19.963 ± 0.086	two 13 min integrations
1997 CS_{29}	1998 Feb 25.4352				19.956 ± 0.062	three 13 min integrations
1997 CS_{29}	1998 Feb 26.3052	43.612	42.883	0.888	20.110 ± 0.088	three 13 min integrations
1997 CS_{29}	1998 Feb 26.4092				20.065 ± 0.172	two 13 min integrations
1997 CS_{29}	1999 Jan 17.4705	43.616	42.633	0.011	19.897 ± 0.049	T_{int} 45 min
1997 CS_{29}	1999 Jan 18.4873	43.616	42.633	0.033	19.774 ± 0.063	two 13 min integrations
1997 CS_{29}	1999 Jan 18.5955				19.948 ± 0.095	T_{int} 13 min
1997 CS_{29}	1999 Jan 19.5819	43.616	42.633	0.056	19.763 ± 0.093	T_{int} 13 min
1997 CS_{29}	1999 Feb 19.2902	43.617	42.798	0.735	19.971 ± 0.089	
1997 CS_{29}	1999 Feb 19.5098				20.070 ± 0.172	T_{int} 18 min
1997 QJ_4	1998 Sept 25.3058	34.752	33.754	0.163	> 22.4	3σ upper limit in 54 min
1997 QJ_4	1998 Sept 26.4969	34.752	33.755	0.185	22.015 ± 0.289	T_{int} 54 min
1997 QJ_4	1998 Sept 26.5624				22.243 ± 0.563	T_{int} 36 min
1998 WH_{24}	1999 Jan 17.3071	42.748	42.265	1.155	19.597 ± 0.049	
1998 WH_{24}	1999 Jan 17.3405				19.595 ± 0.048	
1998 WH_{24}	1999 Jan 18.3232	42.748	42.280	1.166	19.561 ± 0.049	three 13 min integrations
1998 WH_{24}	1999 Jan 19.2648	42.748	42.296	1.177	19.465 ± 0.046	three 13 min integrations
1998 WH_{24}	1999 Feb 19.2491	42.748	42.818	1.320	19.553 ± 0.077	
1998 WH_{24}	1999 Feb 19.3238				19.481 ± 0.064	

TABLE III

H_V Values and Comparison with Different Groups

Object	This work	Jewitt & Luu (1998)	Romanishin & Tegler (1999)
1993 SB	8.26 ± 0.05		
1993 SC	7.38 ± 0.05	7.37 ± 0.04	7.23 ± 0.02
1994 TB	8.04 ± 0.05		7.91-8.17
1995 QY_9	7.98 ± 0.04		7.77-8.37
1996 SZ_4	8.41 ± 0.09		
1996 TL_{66}	5.49 ± 0.02	5.44 ± 0.05	5.40 ± 0.03
1996 TO_{66}	4.71 ± 0.04	4.83 ± 0.03	4.75 ± 0.05
1996 TP_{66}	7.44 ± 0.03	7.54 ± 0.05	7.39 ± 0.06
1996 TQ_{66}	7.51 ± 0.06		7.69 ± 0.11
1996 TS_{66}	6.51 ± 0.06	6.46 ± 0.08	6.50 ± 0.08
1997 CS_{29}	5.54 ± 0.05		5.52 ± 0.11
1997 QJ_4	7.87 ± 0.11		
1998 WH_{24}	4.92 ± 0.04		

The quoted Hv values are derived from the mean of all observations, but do not take account of any lightcurve variations which may be present (e.g. for 1994 TB and 1995 QY9) since we do not know the rotational phase or detailed lightcurve. The values quoted for 1994 TB and 1995 QY_9 represent the range of the reported lightcurves.

TABLE IV

Optical-Infrared (V−J) Colors.

Object	Date	V_{used}	J_{used}	V−J	Note
1993 SB	1998 Sept 25.44	23.170 ± 0.046	> 21.8	< 1.370	3σ limit for J of 21.8
					Simultaneous V
1993 SC	1998 Sept 24.47	22.794 ± 0.046	20.330 ± 0.099	2.464 ± 0.099	Simultaneous V
1993 SC	1998 Sept 24.60	22.663 ± 0.102	20.286 ± 0.178	2.377 ± 0.205	Simultaneous V
1993 SC	1998 Sept 26.53	22.73 ± 0.05	20.187 ± 0.080	2.554 ± 0.090	Using Hv=7.38
1993 SC	1998 Sept 26.59	22.73 ± 0.05	19.937 ± 0.099	2.79 ± 0.11	Cirrus present throughout night
1994 TB	1998 Sept 24.56	22.787 ± 0.095	20.393 ± 0.136	2.394 ± 0.166	Simultaneous V
1994 TB	1998 Sept 25.54	22.797 ± 0.059	20.254 ± 0.089	2.543 ± 0.107	Simultaneous V
1995 QY_9	1998 Sept 24.40	22.690 ± 0.043	20.784 ± 0.123	1.906 ± 0.130	Simultaneous V
1995 QY_9	1998 Sept 24.50	22.673 ± 0.061	20.491 ± 0.154	2.182 ± 0.166	Simultaneous V
1996 SZ_4	1998 Sept 25.41	23.209± 0.089	> 21.8	< 1.409	3σ limit for J of 21.8
					Simultaneous V
1996 TL_{66}	1997 Oct 13.37	20.95 ±0.02	20.045 ± 0.080	0.90 ± 0.080	Using Hv=5.49
1996 TL_{66}	1997 Oct 13.60	20.95 ±0.02	19.850 ± 0.082	1.10 ± 0.082	Using Hv=5.49
1996 TL_{66}	1997 Nov 22.25	20.98 ±0.02	19.734 ± 0.049	1.25 ± 0.049	Using Hv=5.49
1996 TL_{66}	1998 Sept 23.50	21.014 ± 0.009	19.655 ± 0.046	1.359 ± 0.047	Simultaneous V
1996 TL_{66}	1998 Sept 23.61	21.009 ± 0.012	19.445 ± 0.055	1.36 ± 0.056	Simultaneous V
1996 TO_{66}	1998 Sept 23.56	21.284 ± 0.036	20.287 ± 0.094	0.997 ± 0.101	Simultaneous V
1996 TP_{66}	1997 Sept 01.53	21.79 ± 0.03	19.568 ± 0.058	2.20 ± 0.07	Using Hv=7.44
1996 TP_{66}	1997 Oct 13.41	21.61 ± 0.03	19.584 ± 0.113	2.03 ± 0.12	Using Hv=7.44
1996 TP_{66}	1997 Oct 13.57	21.61 ± 0.03	19.690 ± 0.092	1.92 ± 0.10	Using Hv=7.44
1996 TP_{66}	1997 Nov 22.25	21.75 ± 0.03	19.614 ± 0.118	2.141 ± 0.118	Using Hv=7.44
1996 TP_{66}	1998 Sept 25.62	21.697 ± 0.023	19.388 ± 0.056	2.309 ± 0.061	Simultaneous V
1996 TQ_{66}	1998 Sept 23.40	22.947 ± 0.050	20.504 ± 0.099	2.443 ± 0.111	Simultaneous V
1996 TQ_{66}	1998 Sept 23.53	23.152 ± 0.089	20.727 ± 0.118	2.425 ± 0.156	Simultaneous V
1996 TQ_{66}	1999 Jan 18.23	23.15 ± 0.06	20.851 ± 0.159	2.30 ± 0.17	Using Hv=7.57

TABLE IV

Continued.

Object	Date	V_{used}	J	V−J	Note
1996 TS_{66}	1998 Sept 23.46	22.574 ± 0.038	20.736 ± 0.176	1.838 ± 0.180	Simultaneous V
1996 TS_{66}	1998 Sept 23.58	22.415 ± 0.089	20.604 ± 0.150	1.811 ± 0.174	Simultaneous V
1996 TS_{66}	1999 Jan 18.28	22.48 ± 0.06	20.618 ± 0.195	1.86 ± 0.20	Using Hv=6.51
1997 CQ_{29}	1999 Apr 11.37	23.000 ± 0.300	21.159 ± 0.221	1.841 ± 0.373	Assuming Hv=6.7
1997 CS_{29}	1998 Feb 24.34	22.00 ± 0.05	19.997 ± 0.089	2.00 ± 0.10	Using Hv=5.54
1997 CS_{29}	1998 Feb 24.42	22.00 ± 0.05	20.001 ± 0.131	2.00 ± 0.14	Using Hv=5.54
1997 CS_{29}	1998 Feb 24.49	22.00 ± 0.05	19.923 ± 0.092	2.08 ± 0.10	Using Hv=5.54
1997 CS_{29}	1998 Feb 25.30	22.01 ± 0.05	19.963 ± 0.086	2.05 ± 0.10	Using Hv=5.54
1997 CS_{29}	1998 Feb 25.44	22.01 ± 0.05	19.956 ± 0.062	2.05 ± 0.08	Using Hv=5.54
1997 CS_{29}	1998 Feb 26.31	22.01 ± 0.05	20.110 ± 0.088	1.90 ± 0.10	Using Hv=5.54
1997 CS_{29}	1998 Feb 26.41	22.01 ± 0.05	20.065 ± 0.172	1.95 ± 0.18	Using Hv=5.54
1997 CS_{29}	1999 Jan 17.47	22.021 ± 0.056	19.897 ± 0.049	2.124 ± 0.074	Simultaneous V
1997 CS_{29}	1999 Jan 18.49	21.947 ± 0.089	19.774 ± 0.063	2.173 ± 0.109	Simultaneous V
1997 CS_{29}	1999 Jan 18.60	21.814 ± 0.089	19.948 ± 0.095	1.866 ± 0.130	Simultaneous V
1997 CS_{29}	1999 Jan 19.58	21.89 ± 0.05	19.763 ± 0.093	2.213 ± 0.11	Using Hv=5.54
1997 CS_{29}	1999 Feb 19.29	21.89 ± 0.05	19.971 ± 0.089	2.02 ± 0.10	Using Hv=5.54
1997 CS_{29}	1999 Feb 19.51	21.89 ± 0.05	20.070 ± 0.172	1.92 ± 0.18	Using Hv=5.54
1997 QJ_4	1998 Sept 25.31	23.264 ± 0.100	>21.8	<1.464 ± 0.100	3σ limit for J of 21.8 Simultaneous V
1997 QJ_4	1998 Sept 26.50	23.24 ± 0.11	22.015 ± 0.289	1.23 ± 0.31	Assuming Hv=7.87
1997 QJ_4	1998 Sept 26.56	23.24 ± 0.11	22.243 ± 0.563	1.00 ± 0.57	Assuming Hv=7.87
1998 WH_{24}	1999 Jan 17.31	21.359 ± 0.065	19.597 ± 0.049	1.762 ± 0.081	Simultaneous V
1998 WH_{24}	1999 Jan 17.34	21.359 ± 0.065	19.595 ± 0.048	1.764 ± 0.081	Simultaneous V
1998 WH_{24}	1999 Jan 18.32	21.346 ± 0.047	19.561 ± 0.046	1.785 ± 0.067	Simultaneous V
1998 WH_{24}	1999 Jan 19.26	21.35 ± 0.04	19.47 ± 0.05	1.88 ± 0.06	Using Hv=4.92
1998 WH_{24}	1999 Feb 19.26	21.39 ± 0.04	19.553 ± 0.077	1.84 ± 0.09	Using Hv=4.92
1998 WH_{24}	1999 Feb 19.32	21.39 ± 0.04	19.481 ± 0.064	1.91 ± 0.08	Using Hv=4.92

TABLE V

Mean Optical-Infrared (V−J) Colors.

Object	Semi-major axis	class	V−J This work	V−J Jewitt & Luu (1998)
1993 SB	39.75	Plutino	< 1.370	
1993 SC	39.91	Plutino	2.57 ± 0.08	1.97 ± 0.08
1994 TB	39.92	Plutino	2.54 ± 0.11	
1995 QY_9	40.12	Plutino	2.01 ± 0.13	
1996 SZ_4	40.01	Plutino	< 1.409	
1996 TL_{66}	85.20	Scattered	1.37 ± 0.06	1.15 ± 0.08
1996 TO_{66}	43.60	Classical	1.00 ± 0.10	0.72 ± 0.09
1996 TP_{66}	39.88	Plutino	2.11 ± 0.06	2.21 ± 0.07
1996 TQ_{66}	39.77	Plutino	2.41 ± 0.08	
1996 TS_{66}	44.28	Classical	1.83 ± 0.11	1.91 ± 0.09
1997 CQ_{29}	44.90	Classical	1.84 ± 0.37	
1997 CS_{29}	43.84	Classical	2.06 ± 0.03	
1997 QJ_4	39.67	Plutino	1.23 ± 0.31	
1998 WH_{24}	42.80	Classical	1.83 ± 0.03	